# Kinetic Studies of Chlorobenzene Reactions with Hydrogen Atoms and Phenyl Radicals and the Thermochemistry of 1-Chlorocyclohexadienyl Radicals.

Yide Gao and Paul Marshall*

Department of Chemistry, University of North Texas, PO Box 305070, Denton, Texas 76203-5070, USA

*marshall@unt.edu, fax (940) 565-4318

Submitted to the **Reaction Kinetics** colloquium.

**Word count** by Method 1: total of **5587 words**

| | |
|---|---|
| Main text | 3284 words |
| Equations | 334 words |
| Nomenclature | 0 |
| References | 489 words |
| Tables | 0 |
| Figures | 1480 words |

**Abstract**

Atomic H and Cl were monitored by time-resolved resonance spectroscopy in the vacuum ultraviolet, following 193 nm laser flash photolysis of $C_6H_5Cl$ and mixtures with $NH_3$, over 300-1020 K and with Ar bath gas pressures from 30 to 440 mbar. Below 550 K simple exponential decays of [H] were observed, and attributed to addition to form chlorocyclohexadienyl radicals. This addition was reversible over 550 – 630 K and the equilibrium constant was determined by a third law approach. The addition rate constant can be summarized as $(1.51 \pm 0.11) \times 10^{-11} \exp((-1397 \pm 29)/T)$ $cm^3$ $molecule^{-1}$ $s^{-1}$ (300 – 630 K, 1σ uncertainties), and the C-H bond dissociation enthalpy in 1-chlorocyclohexadienyl was determined to be 108.1 ± 3.3 kJ $mol^{-1}$ at 298 K. At higher temperatures the photolysis of chlorobenzene yielded H atoms, which is attributed to the reaction of phenyl with chlorobenzene with a rate constant of $(4.5 \pm 1.8) \times 10^{-10} \exp((-4694 \pm 355)/T)$ $cm^3$ $molecule^{-1}$ $s^{-1}$ over 810 - 1020 K. These and other reaction pathways are discussed in terms of information about the potential energy surface obtained via B3LYP/6-311G(2d,d,p) density functional theory.

## 1. Introduction

Chlorobenzene is a model chlorinated aromatic compound whose high temperature chemistry has been investigated in the context of the destruction of chlorinated waste by incineration or desubstitution by hydrogen, and where potential formation of toxic polychlorinated dibenzodioxins is a concern [1-5]. Chlorine substitution has also been observed to enhance soot formation in shock tube experiments [6]. By contrast to chloroalkanes which typically react via direct abstraction, the reactions of chlorobenzene with radicals could involve a variety of further mechanisms, including stabilized addition, displacement and dissociation or isomerization of a bound intermediate [7]. To complement previous studies involving thermal initiation of chlorobenzene chemistry [1-4,7], we present results obtained in a photochemical system. Direct monitoring of H and Cl atomic concentrations over short time scales helps isolate individual elementary steps, and allows measurement of the thermochemistry of the chlorocyclohexadienyl radical intermediate. Stationary points on potential energy surfaces are characterized via density functional theory to assist identification of the major reaction pathways. The rate constant for H addition to chlorobenzene is measured, along with the first determination of the thermochemistry of 1-chlorocyclohexadienyl. Kinetic information is also obtained about the reaction of phenyl radicals with chlorobenzene, where channels that have been discussed in the literature involve displacement of H and Cl atoms [2-4].

## 2. Experimental Method

The photochemical reactor and application to H and Cl kinetics has been detailed in previous publications [8-11]. Briefly, radicals are generated by pulsed excimer laser photolysis of parent molecules at 193 nm, and their concentration is probed by resonance radiation in the vacuum ultraviolet generated in a microwave discharge. Resonance fluorescence is observed with a solar-blind photomultiplier tube with photon counting, and signals following 1000 - 40000 photolysis pulses, typically at 3-4 Hz, are accumulated in a multichannel scaler. A slow flow of gas (>10 cm $s^{-1}$) replenishes the reactants between pulses. Typical time resolutions used are 20-200 μs per channel. H atom fluorescence at 121.6 nm is detected through magnesium fluoride optics and isolated by a dry air filter and an interference filter. Calcium fluoride optics which block Lyman α radiation are used for detection of Cl atom fluorescence at ~130 nm. Ar bath gas at pressures from 30 to 440 mbar serves to thermalize the reactants, ensures constant temperature during the reaction, and slows diffusion to the walls of the reactor. Because the time scale for homogeneous gas-phase chemical reactions is short compared to diffusion times out of the observation zone, surface chemistry plays little role and the reaction system is effectively wall-less.

Experiments are carried out with a large excess of chlorobenzene over radicals, whose concentration is estimated from the photolysis laser intensity and the concentration and UV absorption cross-section of the absorbing species. To avoid secondary chemistry, very low laser fluences of typically 40-200 μJ $cm^{-2}$ were employed. The laser pulse energy *F* was varied to check that the observed kinetics were independent of the initial radical concentration, and that elementary reactions were isolated from subsequent chemistry involving photolysis or reaction products. Chlorobenzene absorbs strongly at 193 nm, and we determined a cross section at room

temperature of $(9.62 \pm 0.14) \times 10^{-18}$ cm$^2$ molecule$^{-1}$. The quantum yield for dissociation to $C_6H_5$ + Cl is unity [12,13].

For a simple kinetic scheme, such as

$$H + C_6H_5Cl \rightarrow C_6H_6Cl \quad (1)$$

$$H \rightarrow \text{loss other than by reaction with } C_6H_5Cl \quad (2)$$

pseudo-first-order conditions apply. $[C_6H_5Cl]$ is effectively constant and [H] follows an exponential decay profile as function of time t, where $[H]=[H]_0 \exp(-k_{ps1} t)$. The pseudo-first-order decay constant is $k_{ps1} = k_1[C_6H_5Cl] + k_2$. $k_1$ is the bimolecular rate constant for reaction 1 and $k_2$ is a sensibly first-order rate coefficient for loss of H out of the observation region in the absence of $C_6H_5Cl$, for example via diffusion. An example decay is shown as the inset of Fig. 1, and $k_{ps1}$ is obtained via a nonlinear least-squares fit to the exponential decay. $k_{ps1}$ is plotted vs. $[C_6H_5Cl]$ to yield $k_1$ as the slope of Fig. 1.

Under some conditions we found the products of reaction 1 decomposed to regenerate H atoms:

$$C_6H_6Cl \rightarrow H + C_6H_5Cl \quad (-1)$$

$$\rightarrow \text{loss without H atom generation} \quad (3)$$

We solved these differential equations for concentration to obtain

$$[H]=[H]_0 \left[ (\lambda_1+k_{-1}+k_3)e^{(\lambda_1 t)} - (\lambda_2+k_{-1}+k_3)e^{(\lambda_2 t)} \right] / (\lambda_1 - \lambda_2)$$

where

$$\lambda_{1,2}= -[(k_1[C_6H_5Cl]+k_2+k_{-1}+k_3) \pm ( (k_1[C_6H_5Cl]+k_2+k_{-1}+k_3)^2 -4(k_1k_3[C_6H_5Cl]+k_2k_{-1}+k_3k_2))^{1/2}] /2$$

The parameters $k_1' = k_1[C_6H_5Cl]$ , $k_{-1}$, and $k_3$ were derived via nonlinear least-squares fitting of the observed biexponential [H] profiles, with $k_2$ fixed from separate experiments with $NH_3$ alone.

A third kind of behavior was also observed, where no H atoms were generated photolytically but instead they were formed chemically. A proposed kinetic scheme for such conditions is

$$C_6H_5Cl + h\nu \rightarrow C_6H_5 + Cl \quad (4)$$

$$C_6H_5 + C_6H_5Cl \rightarrow \text{biphenyl} + Cl \quad (5a)$$

$$\rightarrow \text{chlorobiphenyl} + H \quad (5b)$$

together with a chemical loss path

$$H + C_6H_5Cl \rightarrow \text{products} \quad (6)$$

which, by contrast to reaction 1, is not addition, and loss of H via (2). The corresponding rate law is

$$[H] = ([H]_0 - \frac{k_{5b}'[C_6H_5]_0}{k_6' + k_2 - k_5'})e^{-(k_6' + k_2)t} + \frac{k_{5b}'[C_6H_5]_0}{k_6' + k_2 - k_5'}e^{-k_5' t}$$

where $k_5 = k_{5a}+k_{5b}$, $k_5' = k_5[C_6H_5Cl]$, $k_6' = k_6[C_6H_5Cl]$, and $k_{5b}' = k_{5b}[C_6H_5Cl]$. The last term, with $k_5' > k_6' + k_2$, corresponds to growth of [H] while the first term corresponds to decay of [H], including any formed in the photolysis pulse ($[H]_0$).

Density functional theory (DFT) calculations were carried out with the Gaussian 03 program suite [14]. Structures were optimized at the B3LYP/6-311G(2d,d,p) level of theory, and vibrational frequencies were scaled by a standard factor of 0.99 [15]. This methodology was chosen because it is insensitive to spin-contamination, with $<S^2>$ below 0.79 for all doublet

species, which is close to the ideal value of 0.75. By contrast, unrestricted Hartree-Fock wavefunctions showed $<S^2>$ up to ~1.4.

## 3. Results and Discussion

Our observations may be divided into three temperature regions. In the low temperature regime, where T ~ 300 - 550 K, simple first order kinetics for reaction of H with $C_6H_5Cl$ were seen, exemplified in Fig. 1, following their generation by photolysis of $NH_3$ precursor. No H atoms were observed in the absence of $NH_3$. The measurements and experimental conditions are summarized in Table S1 of the Supplemental Material. The rate constant $k_1$ was found to be independent, within the experimental scatter, of the average gas residence time in the reactor before photolysis $\tau_{res}$, the laser pulse energy *F*, and the pressure *P*, which is consistent with successful isolation of the kinetics from secondary chemistry and insignificant thermal decomposition of the reactants. The initial radical concentrations $[Cl]_0 = [C_6H_5]_0$ arising from photolysis of chlorobenzene along with the H-atom precursor are given in Table S1. In principle H + phenyl chemistry, which has a high rate constant [16], could account for 15-30% of H consumption at room temperature, 7-20% at 363 K and less than 5% at 630 K. These are pessimistic estimates that ignore consumption of phenyl by, for example, reaction with Cl or chlorobenzene. The observed independence of $k_1$ from $[Cl]_0 = [C6H5]_0$ indicates that any such interference from H + phenyl was minor.

$k_1$ is plotted in Arrhenius form on Fig. 2, and may be expressed as $k_1 = (1.51 \pm 0.11) \times 10^{-11}$ $\exp((-1397 \pm 29)/T)$ $cm^3$ $molecule^{-1}$ $s^{-1}$ (1σ uncertainties). There is one prior measurement of the H-atom reaction with chlorobenzene at below ~600 K, conducted by Sauer and Mani who

employed pulsed radiolysis followed by time-resolved UV absorption to monitor the product at wavelengths of ca. 300 - 330 nm over 298 - 393 K [17]. The comparison on Fig. 2 indicates very close agreement between these two different methods to measure $k_1$.

$k_1$ is a factor of 3 higher than the analogous H + $C_6H_6$ rate constant at room temperature, and similar to this rate constant at 500 K [18]. The benzene reaction proceeds via addition to make cyclohexadienyl and is at the high-pressure limit at 10 Torr of Ar bath gas. Probing for Cl atoms indicated no chemical production of Cl after the photolysis pulse, which rules out a major contribution from a Cl-atom displacement pathway. Photolytically-formed Cl was observed to decay at rates up to ~100 $s^{-1}$, which we attribute to reaction with phenyl radicals [19]. Cl abstraction by H, as argued below from computational results, is too slow to contribute significantly, less than 5% in this low temperature regime. Thus a plausible interpretation is that the H + $C_6H_5Cl$ reaction proceeds via addition to one of the carbon atoms, like H + $C_6H_6$. Unlike in the benzene system, several chlorocyclohexadienyl isomers are possible depending on where the H atom adds relative to the Cl atom in chlorobenzene:

$$H + C_6H_5Cl\ (+ M) \rightarrow \text{6-chlorocyclohexadienyl } (+ M) \quad (7a)$$

$$\rightarrow \text{1-chlorocyclohexadienyl } (+ M) \quad (7b)$$

$$\rightarrow \text{2-chlorocyclohexadienyl } (+ M) \quad (7c)$$

$$\rightarrow \text{3-chlorocyclohexadienyl } (+ M) \quad (7d)$$

Fig. 3 shows paths to these isomers together with the 0 K energies (including zero-point vibrational energy) of the corresponding transition states (TSs), $E_0$, derived via DFT. Details of the computational data are given in Table S2. It may be seen that the most stable species is

6-chlorocyclohexadienyl, which results from *ipso* addition of H to the C atom bonded to Cl with a barrier of ~32 kJ mol$^{-1}$. The addition paths (7b-7d) at the other C atoms, which are *ortho, meta* and *para*, respectively, to the C-Cl bond, are computed to have lower barriers, in the range 15-17 kJ mol$^{-1}$, and the most kinetically favored product, by a small margin, is where H adds *ortho* to the C-Cl bond. The resulting 1-chlorocyclohexadienyl product is also, by a small amount, computed to be the most stable of the adducts where H is not bonded to the halogenated C atom. A transition state theory (TST) analysis[20,21]

$$k = \Gamma \ell \frac{k_B T}{h} \frac{Q_{TS}}{Q_{\text{reactants}}} e^{-\frac{E_0}{RT}}$$

for this path yields the high-pressure limit for addition, with molecular partition functions Q derived from the DFT data in Table S2. Inclusion of the reaction path degeneracy $\ell = 4$ (and equivalently leaving out symmetry factors for rotation and optical isomers) leads to $k_{7b} = 1.4 \times 10^{-15}\ T^{1.54} \exp(-1189/T)$ cm$^3$ molecule$^{-1}$ s$^{-1}$. This theoretical expression for 250 - 2000 K includes a Wigner tunneling correction $\Gamma$ [20] which is modest, and for example $\Gamma$ equals a factor of 1.5 at room temperature, decreasing to 1.05 at 1000 K. Kinetic contributions from the other two pathways (7c and 7d) are likely, and TST yields $k_{7c} = 1.2 \times 10^{-15}\ T^{1.55} \exp(-1373/T)$ cm$^3$ molecule$^{-1}$ s$^{-1}$ and $k_{7d} = 6.1 \times 10^{-16}\ T^{1.55} \exp(-1236/T)$ cm$^3$ molecule$^{-1}$ s$^{-1}$, with reaction path degeneracies of 4 and 2, respectively. The total addition rate constant is $k_{7b} + k_{7c} + k_{7d} = 2.8 \times 10^{-15}\ T^{1.56} \exp(-1246/T)$ cm$^3$ molecule$^{-1}$ s$^{-1}$. This is in order-of magnitude accord with our measurements: the DFT data overestimate the combined addition path by about a factor of 2 at 300 K and a factor of 5 at 600 K. By analogy with H + $C_6H_6$, the addition channels (7b-7d) will be at their high-pressure limits under our experimental conditions. We note that the significant

barrier of ~111 kJ mol$^{-1}$ relative to H + $C_6H_6$ for 1,2 H-shifts in cyclohexadienyl [22] means that these channels are distinct.

*Ipso* addition via TS7a in Fig. 3 in fact corresponds to a displacement pathway, because the initially energized 6-chlorocyclohexadienyl intermediate can rapidly eliminate atomic Cl:

$$H + C_6H_5Cl \rightarrow \text{6-chlorocyclohexadienyl*} \rightarrow Cl + C_6H_6 \qquad (8)$$

Under our conditions the kinetics are insensitive to the C-Cl bond strength in this species, and whether it is a pi or sigma bonded adduct [23], because its dissociation is not rate limiting for pathway (8) and the effective rate coefficient for Cl atom production at moderate pressures will be $k_{7a}$ [4], which from DFT and TST is predicted to be $1.8 \times 10^{-16}\ T^{1.64}\ \exp(-2911/T)$ cm$^3$ molecule$^{-1}$ s$^{-1}$. This is much smaller than the rate constant for addition, $k_1$. Consistent with this calculation, no signal arising from growth in [Cl] due to chemical reaction (upper limit ~5%) was seen after photolysis when the system was probed with a Cl resonance lamp. On the other hand, there was extensive Cl formation during photolysis which, along with the observed lack of H formation, is consistent with the idea that channel (4) is the dominant photochemical process at 193 nm [12,13].

H-atom abstraction has a predicted DFT barrier of 46-52 kJ mol$^{-1}$ (Table S2) depending on the site attacked. This is the least favorable reaction path for H reaction with $C_6H_5Cl$ and is not therefore considered further here.

In an intermediate temperature region with T ~ 580 - 635 K, biexponential decays of [H] were seen, following its generation by photolysis of $NH_3$ precursor. An example is shown as the inset in Fig. 4. We interpret this behavior in terms of reversible adduct formation, where at sufficiently high temperatures cyclohexadienyl-like radicals will decompose by H-atom elimination. We

analyzed such decays according to the scheme of reactions (1), (2), (-1) and (3) to obtain $k_1$, $k_{-1}$ and $k_3$. In general, biexponential analysis is potentially ill-conditioned, so it is important to check the consistency of the derived parameters. As may be seen in the example run shown in Fig. 4, the loss of adduct is independent of [$C_6H_5Cl$], i.e., it is verified to be first-order at fixed total pressure, and redissociation (by H elimination, $k_{-1}$) is the major path while loss without H generation ($k_3$) is minor. Similarly, the main consumption of H is first-order in [$C_6H_5Cl$] ($k_1$) and the contribution from path (2) is minor. The results are summarized in Table S1.

The ratio of these rate constants is the equilibrium constant $K_{eq}$ for adduct formation and, after conversion of $K_{eq}$ to a standard state of $10^5$ Pa, our data are plotted in van't Hoff form in Fig. 5. A "third law" analysis was used, where the intercept was constrained to $\Delta S_{298}/R = 10.97$ derived from the DFT parameters. ln $K_{eq}$ includes a small correction of about 0.2, derived via $-(\Delta S_T - \Delta S_{298})/R + (\Delta H_T - \Delta H_{298})/RT$, which allows for the temperature dependence of $\Delta S$ and $\Delta H$ (see Table S3). The observed $K_{eq}$ corresponds to reversible formation of the 1-chlorocyclohexadienyl isomer, because the less stable species are already not formed significantly (i.e., they dissociate more rapidly) at the highest temperatures where biexponential decays were seen. In other words, at the limiting temperatures where reversible equilibrium is observed, only the most stable isomer contributes. The slope of Fig. 5 yields $\Delta H_{298} = 108.1$ kJ mol$^{-1}$, which corresponds to the C-H bond dissociation enthalpy in 1-chlorocyclohexadienyl. More rigorously, it corresponds to a quantity averaged over the isomers and dominated by the most stable species. Allowance for a factor of 2 uncertainty in $K_{eq}$ in Fig. 5 leads to an error limit of about ±3.3 kJ mol$^{-1}$. The computed DFT value of $\Delta H_{298} = 104.4$ kJ mol$^{-1}$, derived from the 0 K absolute energies in Table S2 and the thermal corrections from Table S3, is in good accord with this measured $\Delta H_{298}$, which lends support to our interpretation. There is no prior determination of the thermochemistry of

chlorocyclohexadienyl, but we note that the C-H bond dissociation enthalpy found here is not significantly different from that in cyclohexadienyl, 109.6 ± 11.7 kJ mol$^{-1}$ [18]. The H-$C_6H_4Cl$ bond strength together with $\Delta_fH_{298}$ for H and $C_6H_5Cl$ of 218.0 and -54.4 ± 0.9 kJ mol$^{-1}$, respectively [24], yields $\Delta_fH_{298}$(1-$C_6H_6Cl$) = 271.7 ± 3.4 kJ mol$^{-1}$.

In the high temperature regime T ~ 800-1000 K, H atoms were observed during photolysis of chlorobenzene in the absence of added $NH_3$ precursor. The yield of H increased with temperature, and at lower temperatures (~ 650 – 700 K) was too small to use for kinetic analysis. A typical fluorescence profile is shown in Fig. 6. Atomic hydrogen is not formed by direct photolysis, but is seen to grow through chemical reaction. A possible scheme involves reaction (5b), where photolytically produced $C_6H_5$ reacts with chlorobenzene to produce, at least in part, H atoms. The rate of growth of [H] yields the combined rate constant $k_5 = k_{5a} + k_{5b}$ which is plotted in Arrhenius form in Fig. 7. $k_5$ can be expressed, over 810-1020 K, as $k_5 = (4.5 \pm 1.8) \times 10^{-10} \exp((-4694 \pm 355)/T)$ cm$^3$ molecule$^{-1}$ s$^{-1}$. Also shown in the Arrhenius plot are the 1973 estimates of Louw and coworkers for channels (5a) and (5b) [7], who assumed $k_{5b}$ was similar to their empirically estimated phenyl + benzene rate constant [25]. In accord with our lack of observation of Cl atom growth, they set $k_{5a} \sim 0.1\ k_{5b}$, but the absolute magnitude of their rate constants is about two orders of magnitude smaller than determined here. This difference arises mainly from their smaller pre-exponential factor of $1.7 \times 10^{-13}$ cm$^3$ molecule$^{-1}$ s$^{-1}$ for the dominant $k_{5b}$ path, which corresponds to a tighter transition state. The analogous phenyl + benzene rate constant has been recently reassessed as about 4 times larger at 800 K [26], which reduces the discrepancy.

After generation of atomic H, its concentration then falls slowly, at of the order of 10 s$^{-1}$, and for fitting purposes this loss is ascribed an effective second-order rate constant $k_6$. The results from

this analysis are summarized in Table S4. We do not interpret the overall loss (6) as an elementary reaction. The data for $k_6$ are highly scattered, with an uncertainty comparable to the magnitude of $k_6$, but they indicate that $k_6 < 10^{-13}$ cm$^3$ molecule$^{-1}$ s$^{-1}$. If overall loss (6) corresponded to one or more elementary paths, its rate constant would have to be at least equal to that for Cl-atom abstraction

$$H + C_6H_5Cl \rightarrow C_6H_5 + HCl \qquad (9)$$

The DFT data yield a TST rate constant of $k_9 = 4.4 \times 10^{-15}\ T^{1.55} \exp(-4340\ K/T)$ cm$^3$ molecule$^{-1}$ s$^{-1}$. This expression yields rate constants of $6 \times 10^{-13}$ and $3 \times 10^{-12}$ cm$^3$ molecule$^{-1}$ s$^{-1}$ at 800 and 1000 K, respectively, showing that $k_9 > k_6$. Similarly, $k_6$ would have to be at least equal to $k_{7a} = k_8$ for Cl-atom displacement, but the DFT data yield rate constants $k_8$ of $3 \times 10^{-13}$ and $8 \times 10^{-13}$ cm$^3$ molecule$^{-1}$ s$^{-1}$ at 800 and 1000 K, respectively, showing that $k_8 > k_6$. We speculate that the overall loss of H is slowed by a chain reaction, where step (9) is followed by regeneration of H through reaction (5b). Also, chlorophenyl species, generated by abstraction of H from $C_6H_5Cl$ by atomic Cl, may react with chlorobenzene analogously to phenyl in steps 5a and 5b, which will further replenish [H] and lead to small net loss rates of atomic H. The observed loss rates of atomic Cl at around 1000 K are consistent with a rate constant for Cl + $C_6H_5Cl$ reaction of about $10^{-12}$ cm$^3$ molecule$^{-1}$ s$^{-1}$. Quantitative modeling of this chemistry will be addressed in a future study.

## 4. Conclusions

At temperatures below 630 K, the dominant path for the H + $C_6H_5Cl$ reaction is addition to make stabilized chlorocyclohexadienyl radicals. These adducts become unstable at the upper end of

this range, and observation of reversible adduct formation yields the C-H bond dissociation enthalpy. At higher temperatures more complex behavior is seen. H atoms are formed chemically, which is attributed to the reaction of phenyl with chlorobenzene. No evidence for Cl formation was seen, although a minor branching ratio cannot be ruled out. Net loss of H atoms is very slow, and potential H-atom regeneration processes include displacement reaction of phenyl and chlorophenyl radicals, formed by attack of atomic Cl, with chlorobenzene.

**Acknowledgments**

This work was supported by the Robert A. Welch Foundation (Grant B-1174) and the UNT Faculty Research Fund. The laser and computational facilities were purchased with NSF grants CTS-0113605 and CHE-0342824, respectively.

## References


[1] J. A. Manion, P. Mulder and R. Louw, Environ. Sci. Technol. 19 (1985) 280.

[2] J. A. Manion and R. Louw, J. Phys. Chem. 94 (1990) 4127.

[3] J. P. Cui, Y. Z. He and W. Tsang, J. Phys. Chem. 93 (1989) 724.

[4] E. R. Ritter, J. W. Bozzelli and A. M. Dean, J. Phys. Chem. 94 (1990) 2493.

[5] B. R. Stanmore, Combust. Flame 136 (2004) 398.

[6] M. Frenklach, M. Ramachandra and A. Matula, Proc. Combust. Inst. 20 (1984) 871.

[7] R. Louw, J. W. Rothuizen and R. C. C. Wegman, J. Chem. Soc. Perkin Trans. II (1973) 1635.

[8] L. Ding and P. Marshall, J. Phys. Chem. 96 (1992) 2197.

[9] A. Goumri, W.-J. Yuan, L. Ding, Y. Shi and P. Marshall, Chem. Phys. 177 (1993) 233.

[10] J. Peng, X. Hu and P. Marshall, J. Phys. Chem. A 103 (1999) 5307.

[11] I. M. Alecu, Y. Gao, P.-C. Hsieh, J. P. Sand, A. Ors, A. McLeod and P. Marshall, J. Phys. Chem. A 111 (2007) 3970.

[12] T. Ichimura and Y. Mori, J. Chem. Phys. 58 (1973) 288.

[13] T. Ichimura, Y. Mori, H. Shinohara and N. Nishi, Chem. Phys. Lett. 189 (1994) 117.

[14] M. J. Frisch, G. W. Trucks, H. B. Schlegel, G. E. Scuseria, M. A. Robb, J. R. Cheeseman, J. J. A. Montgomery, T. Vreven, K. N. Kudin, J. C. Burant, J. M. Millam, S. S. Iyengar, J. Tomasi, V. Barone, B. Mennucci, M. Cossi, G. Scalmani, N. Rega, G. A. Petersson, H. Nakatsuji, M. Hada, M. Ehara, K. Toyota, R. Fukuda, J. Hasegawa, M. Ishida, T. Nakajima, Y. Honda, O. Kitao, H. Nakai, M. Klene, X. Li, J. E. Knox, H. P. Hratchian, J. B. Cross, C. Adamo, J. Jaramillo, R. Gomperts, R. E. Stratmann, O. Yazyev, A. J. Austin, R. Cammi, C. Pomelli, J. W. Ochterski, P. Y. Ayala, K. Morokuma, G. A. Voth, P.

Salvador, J. J. Dannenberg, V. G. Zakrzewski, S. Dapprich, A. D. Daniels, M. C. Strain, O. Farkas, D. K. Malick, A. D. Rabuck, K. Raghavachari, J. B. Foresman, J. V. Ortiz, Q. Cui, A. G. Baboul, S. Clifford, J. Cioslowski, B. B. Stefanov, G. Liu, A. Liashenko, P. Piskorz, I. Komaromi, R. L. Martin, D. J. Fox, T. Keith, M. A. Al-Laham, C. Y. Peng, A. Nanayakkara, M. Challacombe, P. M. W. Gill, B. Johnson, W. Chen, M. W. Wong, C. Gonzalez and J. A. Pople, Gaussian 03. Gaussian, Pittsburgh, 2003.

[15] J. A. Montgomery, Jr., M. J. Frisch, J. W. Ochterski and G. A. Petersson, J. Chem. Phys. 110 (1999) 2822.

[16] L. B. Harding, Y. Georgievskii and S. J. Klippenstein, J. Phys. Chem. A 109 (2005) 4646.

[17] M. C. Sauer, Jr. and I. Mani, J. Phys. Chem. 74 (1970) 59.

[18] J. M. Nicovich and A. R. Ravishankara, J. Phys. Chem. 88 (1984) 2534.

[19] K. Tonokura, Y. Norikane, M. Koshi, Y. Nakano, S. Nakamichi, M. Goto, S. Hashimoto, M. Kawasaki, M. P. S. Anderson, M. D. Hurley and T. J. Wallington, J. Phys. Chem. A 106 (2002) 5908.

[20] M. F. R. Mulcahy Gas Kinetics, Nelson, London, 1973.

[21] R. G. Gilbert and S. C. Smith Theory of Unimolecular and Recombination Reactions, Oxford University Press, Oxford, 1990.

[22] I. V. Tokmakov and M. C. Lin, Int. J. Chem. Kinet. 33 (2001) 633.

[23] A. K. Croft and H. M. Howard-Jones, Phys. Chem. Chem. Phys. 9 (2007) 5649.

[24] V. A. Platonov and Y. N. Simulin, Zhurnal Fizicheskoi Khimii 59 (1985) 300.

[25] R. Louw and H. J. Lucas, Rec. Trav. Chim. 92 (1973) 55.

[26] J. Park, S. Burova, A. S. Rodgers and M. C. Lin, J. Phys. Chem. A 103 (1999) 9036.

**Figure captions**

Fig. 1 Plot of pseudo-first-order decay coefficient for [H] vs. [$C_6H_5Cl$] at 363 K and 156 mbar total pressure. The inset shows the fluorescence decay for the highlighted point.

Fig. 2 Arrhenius plot for addition of H to [$C_6H_5Cl$]. Solid line: this work; dashed line: ref. [17].

Fig. 3 Potential energy diagram for H + $C_6H_5Cl$ derived from B3LYP/6-311G(2d,d,p) data.

Fig. 4 Plot of first-order rate constants for H + $C_6H_5Cl$ at 580 K and 157 mbar Ar pressure. Circles: consumption of H by addition to $C_6H_5Cl$ and other processes independent of [$C_6H_5Cl$] such as diffusion ($k_1$[$C_6H_5Cl$] + $k_2$); triangles: dissociation of adduct to H + $C_6H_5Cl$ ($k_{-1}$); stars: loss of adduct not creating H, ($k_3$). The inset shows a biexponential fluorescence decay corresponding to the filled point.

Fig. 5 van't Hoff plot for H addition to $C_6H_5Cl$. The intercept is constrained to the B3LYP/6-311G(2d,d,p) value of $\Delta S_{298}/R$. The inset shows an enlargement of the area around the measurements.

Fig. 6 Growth and decay of [H] following photolysis of $C_6H_5Cl$ at 1023 K and 315 mbar Ar. The reaction of phenyl with chlorobenzene is described by $k_5' = (k_{5a}+k_{5b})$[$C_6H_5Cl$] (see text).

Fig. 7 Rate constants for phenyl + chlorobenzene reaction. Solid line and points: this work, two channels combined; dashed line: ref. [7] H-atom formation channel; dotted line: ref. [7] Cl-atom formation channel.

Fig. 1 Plot of pseudo-first-order decay coefficient for [H] vs. [$C_6H_5Cl$] at 363 K and 156 mbar total pressure. The inset shows the fluorescence decay for the highlighted point.

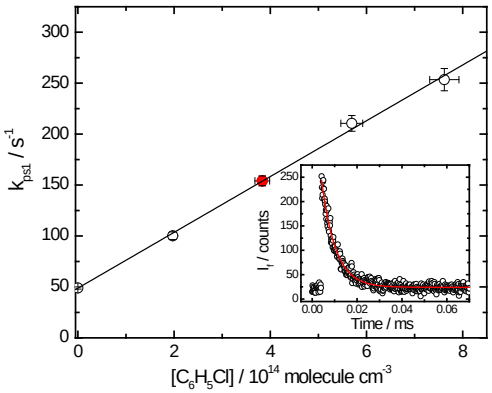


Fig. 2 Arrhenius plot for addition of H to [$C_6H_5Cl$]. Solid line: this work; dashed line: ref. [17].

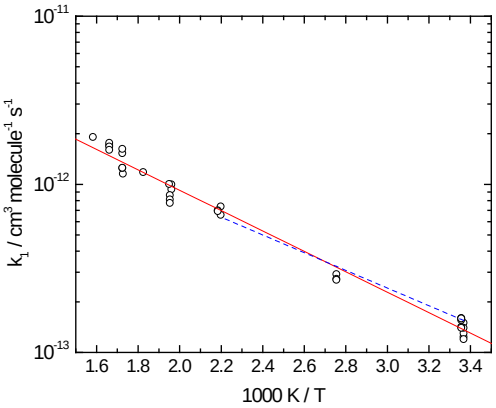

Fig. 3 Potential energy diagram for H + $C_6H_5Cl$ derived from B3LYP/6-311G(2d,d,p) data. Transition states are labeled by the reaction number in the text.

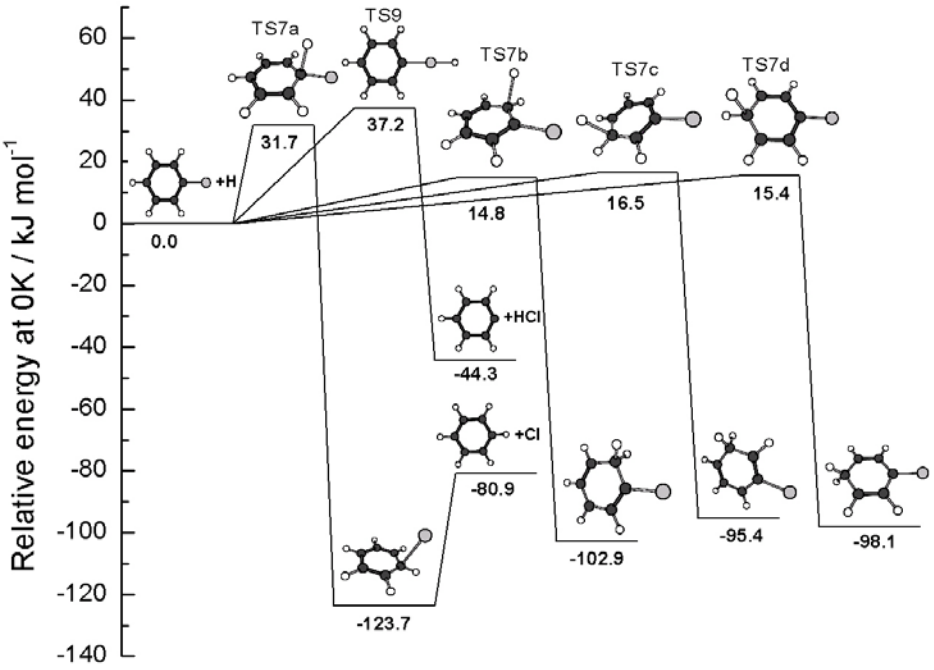

Fig. 4 Plot of first-order rate constants for H + $C_6H_5Cl$ at 580 K and 157 mbar Ar pressure. Circles: consumption of H by addition to $C_6H_5Cl$ and other processes independent of [$C_6H_5Cl$] such as diffusion ($k_1$[$C_6H_5Cl$] + $k_2$); triangles: dissociation of adduct to H + $C_6H_5Cl$ ($k_{-1}$); stars: loss of adduct not creating H, ($k_3$). The inset shows a biexponential fluorescence decay corresponding to the filled point.

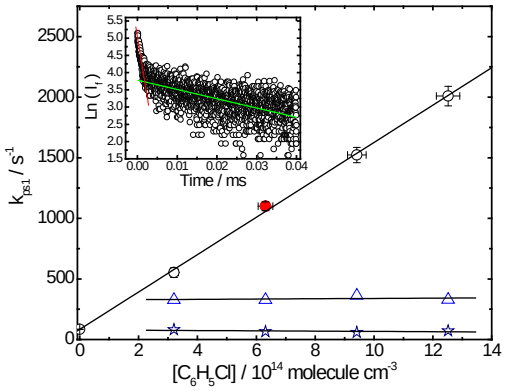


Fig. 5 van't Hoff plot for H addition to $C_6H_5Cl$. The intercept is constrained to the B3LYP/6-311G(2d,d,p) value of $\Delta S_{298}/R$. The inset shows an enlargement of the area around the measurements.

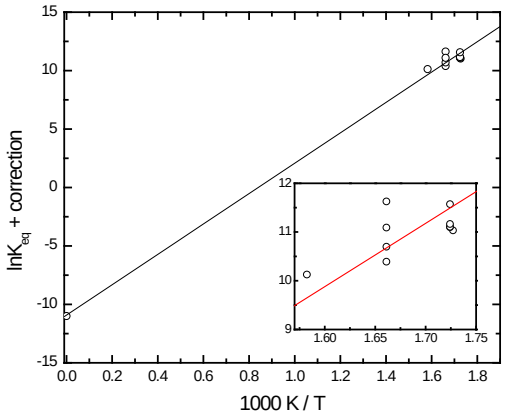

Fig. 6 Growth and decay of [H] following photolysis of $C_6H_5Cl$ at 1023 K and 315 mbar Ar. The reaction of phenyl with chlorobenzene is described by $k_5' = (k_{5a}+k_{5b})[C_6H_5Cl]$ (see text).

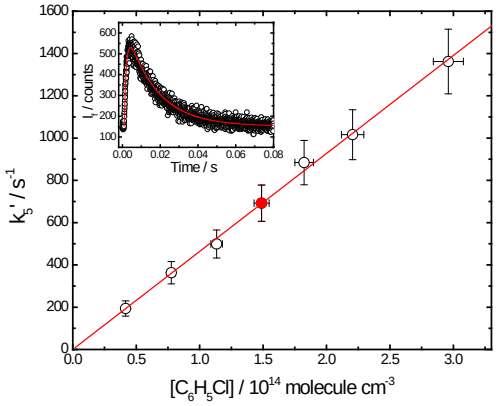


Fig. 7 Rate constants for phenyl + chlorobenzene reaction. Solid line and points: this work, two channels combined; dashed line: ref. [7] H-atom formation channel; dotted line: ref. [7] Cl-atom formation channel.

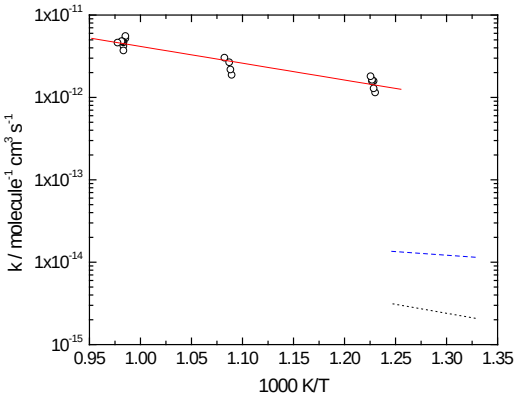

# Supplementary material

Table S1. Summary of kinetic measurements for H + $C_6H_5Cl$ below 635 K.

Table S2. B3LYP/6-311G(2d,d,p) density functional results for the $C_6H_5Cl$+H reaction system.

Table S3. Thermodynamic functions for $C_6H_5Cl$, 1-$C_6H_6Cl$ and $C_6H_5$ based on B3LYP/6-311G(2d,d,p) frequencies and rotational constants.

Table S4. Summary of measurements of the rate constants for phenyl reaction with chlorobenzene, $k_{5a}$ + $k_{5b}$, and effective $k_6$ for H-atom loss in the presence of chlorobenzene, expressed as a second-order rate constant.